ChemComm

COMMUNICATION

View Article Online
View Journal | View Issue

Cite this: *Chem. Commun.*, 2017, 53, 3717

Received 26th January 2017,
Accepted 9th March 2017

DOI: 10.1039/c7cc00736a

rsc.li/chemcomm

Efficient energy transfer between coronene-modified permethyl-β-cyclodextrins and porphyrin for light induced DNA cleavage†

Jie Yu,[a] Ying-Ming Zhang,[a] Pei-Yu Li[a] and Yu Liu*[ab]

A novel supramolecular assembly was constructed by the non-covalent complexation of hexa-*cata*-hexabenzocoronene modified permethyl-β-cyclodextrins with tetrasodium tetraphenylporphyrin-tetrasulfonate in water, exhibiting highly efficient excited energy transfer behaviors and a promising DNA photocleavage ability.

The fabrication of nanometer-scaled architectures with unique structures and function is a crucial aspect in supramolecular chemistry and nanoscience. In this regard, nanographenes synthesized *via* a "bottom-up" method have attracted considerable attraction because of their special structural and physical properties.[1] It is generally recognized that hexa-*peri*-hexabenzocoronene (PHBC) and hexa-*cata*-hexabenzocoronene (CHBC) occupy key positions in the study of nanographenes.[2] Taking advantage of the intrinsic properties of PHBC and CHBC, including intermolecular π–π stacking behaviors and superior electronic performance, many supramolecular architectures have been elaborately constructed and have shown inventive applications in the areas of electronic devices,[3] bioimaging,[4] and chemical sensing.[5]

As an important class of organic dyes, porphyrins have been explored as functional building blocks due to their excellent electroactive and photochemical properties.[6] Many endeavors have been devoted to the covalent combination of hexabenzocoronenes with porphyrins. For instance, the first PHBC–porphyrin triad was synthesized by Wong *et al.* and applied as a photovoltaic device.[7] Hirsch and Jux *et al.* reported a covalently linked PHBC–porphyrin conjugate and Drewello and Jux *et al.* reported a porphyrin derivative with two PHBC units and explored the absorption and emission features of such superbenzene–porphyrin conjugates.[8,9] However, in contrast to these known PHBC–porphyrin systems, there is a relative paucity of studies on the structure–activity relationship of CHBC–porphyrin systems, especially in a noncovalent binding manner. In previous studies, we have presented a series of biocompatible nanocarriers and photo-modulated nanoassemblies based on CD–porphyrin conjugation.[10,11] In the wake of these fascinating results obtained by us and other researchers, we herein report a CHBC derivative (CHBC-1) bearing three permethyl-β-cyclodextrins (PMCDs), which endowed the CHBC core with good water solubility.[12] Moreover, taking advantage of the strong binding ability of PMCD with sulfonated porphyrin,[13] a supramolecular network was constructed in aqueous solution. Moreover, an efficient energy transfer process from CHBC-1 to porphyrin occurred in this artificial nanoassembly, and more significantly, the obtained nanoassembly exhibited excellent DNA photocleavage activity.

Alkynyl-substituted CHBC derivative **4** was synthesized according to the reported literature with a slight modification.[14] Then, permethyl-β-CDs (PMCDs) were grafted onto a CHBC core *via* the Cu(I)-catalyzed Huisgen 1,3-dipolar cycloaddition (Scheme 1). The obtained host compound CHBC-1 was comprehensively characterized by ^{1}H, ^{13}C NMR, and HR-MALDI-TOF spectroscopy (Fig. S1–S3 in the ESI†). Owing to the strong binding affinity of TPPSS with the PMCD cavity, the binary CHBC-1/TPPSS

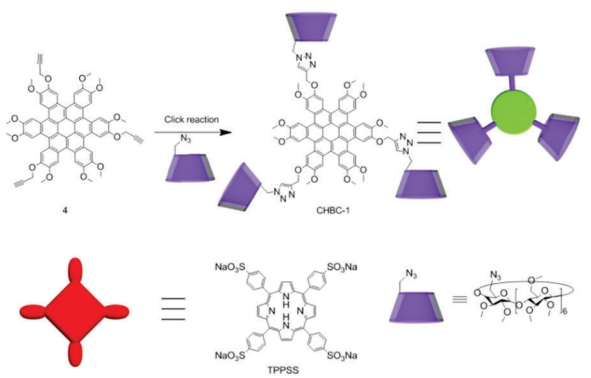

Scheme 1 Synthesis of CHBC-1 and the structure of TPPSS.

[a] *Department of Chemistry, State Key Laboratory of Elemento-Organic Chemistry, Nankai University, Tianjin 300071, P. R. China*
[b] *Collaborative Innovation Center of Chemical Science and Engineering (Tianjin), Nankai University, Tianjin 300071, P. R. China. E-mail: yuliu@nankai.edu.cn*

† Electronic supplementary information (ESI) available: Synthesis and characterization of multifunctional supramolecular conjugates and experimental details. See DOI: 10.1039/c7cc00736a

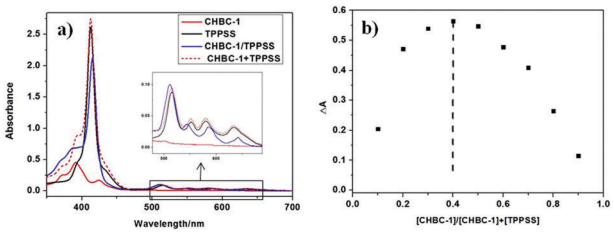

Fig. 1 (a) UV/Vis absorption spectra of CHBC-1, TPPSS, and CHBC-1/TPPSS ([CHBC-1] = 4×10^{-6} M, [TPPSS] = 6×10^{-6} M). Inset: Magnified area of Q-band of TPPSS; and (b) Job plot for CHBC-1 upon complexation with TPPSS in pH = 7.2 phosphate buffer (absorption changes recorded at 412 nm for TPPSS; [CHBC-1] + [TPPSS] = 5×10^{-6} M).

supramolecular assembly could be easily fabricated by mixing CHBC-1 with TPPSS in aqueous solution, which was sufficiently characterized by spectroscopic and microscopic investigation, as described below.

As shown in Fig. 1a, the absorption peaks centered at 278, 390, and 424 nm were assigned to the absorption spectral features of CHBC-1. This information, along with the compound characterization data, jointly confirmed that CHBC-1 was successfully synthesized.[11–15] Meanwhile, by comparing the spectral superposition of CHBC-1 and TPPSS, the absorption peak of the CHBC-1/TPPSS complex showed a bathochromic shift from 412 to 416 nm. Circular dichroism experiments provided additional evidence on the noncovalent association between CHBC-1 and TPPSS. That is, both CHBC-1 and the CHBC-1/TPPSS complex gave negative circular dichroism signals, whereas the assembly's circular dichroism signals were more intensive than CHBC-1 and TPPSS around 386 and 412 nm (Fig. S4 in the ESI†). Since coronene was not a chiral molecule, the well-defined circular dichroism signal of CHBC-1 was obviously attributed to the PMCD-induced circular dichroism. These spectroscopic phenomena jointly suggest that TPPSS was included into the hydrophobic cavity of PMCD. As shown in Fig. S19 (ESI†), the inflection point occurred at a molar fraction of 0.33, corresponding to a 2 : 1 complexation stoichiometry between PMCD and TPPSS.[13] Subsequently, the complexation stoichiometry of CHBC-1 with TPPSS was also identified using a Job plot, where the inflection point occurred at a molar fraction of 0.4, indicating a 2 : 3 complexation stoichiometry (Fig. 1b). Meanwhile, the curve of the absorbance intensity *versus* the [CHBC-1]/[TPPSS] molar ratio showed an inflection point at a molar ratio of 0.67, further suggesting the formation of a host–guest complex in a 2 : 3 molar ratio (Fig. S5 in the ESI†). Although it was not easy to directly obtain the binding constant between CHBC-1 and TPPSS in a 2 : 3 complexation stoichiometry, it is known that the TPPSS/PMCD complex was stable enough to fabricate various functional supramolecular assemblies in water.[6,10,11,13b,16a] Thus, we can also reasonably speculate that the CHBC-1/TPPSS complex in our case would stably exist in aqueous solution.

The noncovalent complexation of CHBC-1 with TPPSS was also investigated by means of NMR spectroscopy. As shown in Fig. S6 (ESI†), the ^{1}H NMR spectrum of CHBC-1 in $CDCl_3$ was distinctly different from the one in D_2O. As judged from the 2D NOESY spectrum in $CDCl_3$, the peaks at 8.78–8.93 and 7.90 ppm could be assigned to the protons of the coronene and triazole rings, respectively (Fig. S7 in the ESI†). According to the NOESY spectra of CHBC-1 in D_2O, the cross-peaks between the protons of coronene and PMCD were observed, indicating that the benzene ring of coronene was self-included into the cavity of PMCD (Fig. S8 in the ESI†).[6a,10] The optimized molecular modulation of CHBC-1 also corroborated that CHBC-1 existed in the self-included conformation in aqueous solution (Fig. S9 in the ESI†). In the CHBC-1/TPPSS complex, the phenyl protons of TPPSS at 7.6–8.5 ppm exhibited multiple cross-peaks with the PMCD, whereas the previously observed cross-peaks between the protons of CHBC-1 and PMCD disappeared (Fig. S10 in the ESI†).[6a,10] These NMR results indicated that the CHBC-1 moiety was expelled from the cavity due to the strong binding ability of PMCD with porphyrin derivatives. There was no obvious Tyndall effect in CHBC-1 or TPPSS solution, suggesting that neither CHBC-1 nor TPPSS could be self-assembled to form large-sized aggregates. Comparatively, the CHBC-1/TPPSS assembly exhibited a clear Tyndall effect in solution (Fig. S11 in the ESI†). Meanwhile, the zeta potential value of the assembly was negative, implying that negative charges were located on the surface of the CHBC-1/TPPSS aggregates (Fig. S12 in the ESI†). Furthermore, the morphology of the supramolecular assembly was also characterized by microscopic investigation. As shown in the TEM image, there were two-dimensional netlike nanostructures, and meanwhile, a number of flake-like nanostructures were found in the SEM image (Fig. S13 in the ESI†).

The photophysical behaviors were further investigated in the CHBC-1/TPPSS assembly. The Q-band of TPPSS and the emission spectrum of CHBC-1 are normalized in Fig. 2a. In the 450–700 nm range, the absorption spectrum of TPPSS largely overlapped with the fluorescence emission spectrum of CHBC-1, which indicated that an efficient excited-energy transfer (EET) process might take place in the CHBC-1/TPPSS assembly.[8,9] Subsequently, the EET process in CHBC-1/TPPSS was investigated by fluorescence spectroscopy. When different amounts of TPPSS were added to the CHBC-1 solution, the fluorescence intensity of CHBC-1 was nearly 100% quenched, while the porphyrin emission was observed at the same time (Fig. 3). In control experiments, although both TPPSS and PMCD/TPPSS systems gave fluorescence emission, the emission intensity of the CHBC-1/TPPSS complex was 1.9 times

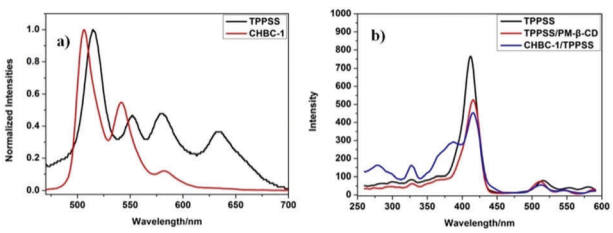

Fig. 2 (a) Normalized spectrum of the Q-band of TPPSS and the emission spectrum of CHBC-1 in phosphate buffer (pH 7.2, λ_{ex} = 380 nm) at 25 °C; and (b) excitation spectra of TPPSS and TPPSS/PMCD and CHBC-1/TPPSS complexes by monitoring the emission wavelength at 655 nm ([CHBC-1] = 1×10^{-6} M, [TPPSS] = 1.5×10^{-6} M, [PMCD] = 3×10^{-6} M).

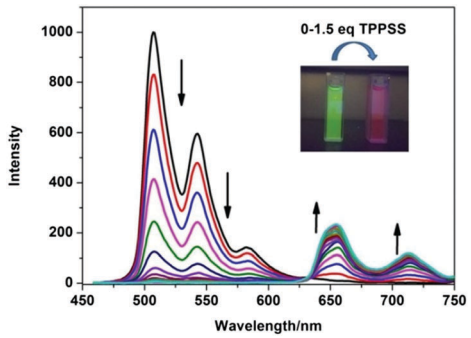

Fig. 3 Fluorescence spectral changes of CHBC-1 upon addition of TPPSS (0–1.5 equiv.) in pH 7.2 phosphate buffer solution at 25 °C ([CHBC-1] = 1×10^{-6} M, λ_{ex} = 380 nm).

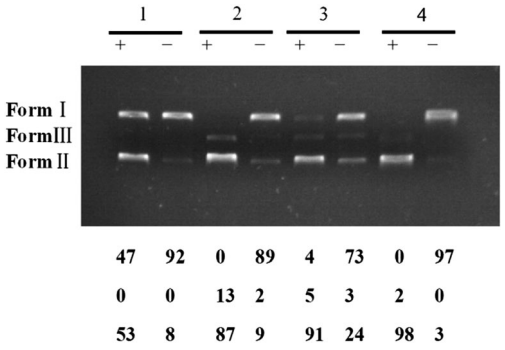

Fig. 4 Photocleavage of pBR322 DNA (5 ng μL^{-1}). Lane 1: the blank control; lane 2: CHBC-1/TPPSS (0.01 mM/0.015 mM); lane 3: CHBC-1 (0.01 mM); lane 4: TPPSS/PMCD systems (0.015 mM/0.02 mM); (+) in the presence and absence (−) of visible light.

greater than the reference groups under the same experimental conditions, implying EET-assisted fluorescence enhancement (Fig. S14 in the ESI†). In our case, the host–guest complexation with the hydrophobic cavity of PMCD could greatly deter the negatively charged porphyrins from self-quenching or solvent attacking, thus leading to different photophysical behaviors as compared to the non-bound porphyrins in water. We further investigated the effect of diffusional collision and no spectral change was observed in **4** or TPPSS when TPPSS was added to a solution of precursor **4** in DMSO (Fig. S15 in the ESI†). These results clearly indicated that the florescence energy could be transferred from excited CHBC-1 to TPPSS moieties in aqueous solution.

In addition, it was found that the excited spectra of CHBC-1/TPPSS, PMCD/TPPSS and TPPSS were similar to their corresponding absorption spectra (Fig. 2b). Although the β band of CHBC overlapped with the Soret band of TPPSS, the excitation and absorption signals of the CHBC-1/TPPSS assembly were more intensive than those of PMCD/TPPSS and TPPSS in the 360–385 nm range. Thus, it is believed that the fluorescence emission of CHBC-1/TPPSS was mainly due to the energy transfer from excited CHBC-1 to TPPSS moieties.

According to Förster's rules,[16] the EET efficiency (E) achieved was 99% in the CHBC-1/TPPSS assembly. Furthermore, in the presence of 1.5 equiv. of TPPSS, the absolute fluorescence quantum yield (Φ) of CHBC-1 decreased from 9.1% to 0.3%. Using the measured Φ, the E value was calculated to be 97%, which was similar to the value obtained above. As shown in Fig. S20 (ESI†), the fluorescence lifetime of CHBC-1 decreased from 23.3 ns to 3.7 ns. Along with the steady fluorescence spectroscopic results, it jointly indicated that the energy transfer from coronene to the porphyrin likely goes through a Förster mechanism. The center distance between the donor (CHBC-1) and acceptor (TPPSS) also played an important role in the EET efficiency.[16a] The distance from the center of CHBC-1 to TPPSS was measured to be 19.9 Å with the optimized molecular modulation from the minimized energy method (Fig. S16 in the ESI†). The following are some reasons for the efficient EET process between CHBC-1 and TPPSS. First, the absorption spectrum of TPPSS largely overlaps with the fluorescence spectrum of CHBC-1. Second, the strong noncovalent interaction between PMCD and TPPSS draws the donor and acceptor together, and the closer center-to-center distance is beneficial for the efficient EET process. Third, the TPPSS moieties were included and protected by the cavity of PMCD, by which the self-quenching or solvent attacking can be avoided to a great extent in water.

Considering that the reactive oxygen species (ROS) can be generated by nanographene and porphyrin, an agarose gel electrophoresis assay was performed to investigate the photo-induced DNA cleavage ability of the CHBC-1/TPPSS supramolecular assembly.[17] As shown in Fig. 4, no DNA cleavage activity was found for CHBC-1/TPPSS, CHBC-1 and PMCD/TPPSS in the dark. In contrast, among all the examined samples, the CHBC-1/TPPSS supramolecular assembly displayed much higher cleavage activity than those of CHBC-1 and PMCD/TPPSS under visible light irradiation (lane 2 in Fig. 4). That is, the closed supercoiled DNA (form I) was completely decomposed to nicked circular DNA (form II, 87%) and linear DNA (form III, 13%). Furthermore, a control experiment was performed to investigate the mechanism of DNA photocleavage. That is, KI, NaN_3 and DMSO were selected as scavengers of hydrogen peroxide, singlet oxygen and hydroxyl radicals, respectively.[18] It was found that the photo-induced DNA cleavage activity of CHBC-1 and the CHBC-1/TPPSS complex was inhibited by NaN_3 and KI, but DMSO was ineffective, suggesting that the hydrogen peroxide and singlet oxygen were the correlative ROS generated by CHBC-1/TPPSS and responsible for the DNA cleavage (Fig. S17 and S18 in the ESI†).

In conclusion, benefiting from the highly affinitive noncovalent binding, a netlike nanographene/porphyrin supramolecular assembly was successfully fabricated from CHBC-modified PMCDs and TPPSS in aqueous solution. Noticeably, an efficient energy transfer was achieved from nanographene to porphyrin in this artificial nanoassembly with a high efficiency of up to 97%. Moreover, the supramolecular assembly exhibited excellent photo-induced DNA cleavage activity. Consequently, the present work not only reveals an excited-energy transfer process in the nanographene/porphyrin supramolecular assembly, but also exhibits the possible application of nanographene/porphyrin conjugation in the field of photodynamic therapy.

We thank the National Natural Science Foundation of China (Grant No. 21432004, 21472100, and 91527301) for financial support.

Notes and references

1 (*a*) M. Ball, Y. Zhong, Y. Wu, C. Schenck, F. Ng, M. Steigerwald, S. Xiao and C. Nuckolls, *Acc. Chem. Res.*, 2015, **48**, 267–276; (*b*) M. Kastler, J. Schmidt, W. Pisula, D. Sebastiani and K. Müllen, *J. Am. Chem. Soc.*, 2006, **128**, 9526–9534; (*c*) K. Müllen and J. P. Rabe, *Acc. Chem. Res.*, 2008, **41**, 511–520; (*d*) C.-Y. Chiu, B. Kim, A. A. Gorodetsky, W. Sattler, S. Wei, A. Sattler, M. Steigerwald and C. Nuckolls, *Chem. Sci.*, 2011, **2**, 1480–1486.

2 (*a*) L. Chen, Y. Hernandez, X. Feng and K. Müllen, *Angew. Chem., Int. Ed.*, 2012, **51**, 7640–7654; (*b*) J. Wu, W. Pisula and K. Müllen, *Chem. Rev.*, 2007, **107**, 718–747; (*c*) A. Narita, X.-Y. Wang, X. Feng and K. Müllen, *Chem. Soc. Rev.*, 2015, **44**, 6616–6643.

3 (*a*) L. Chen, K. S. Mali, S. R. Puniredd, M. Baumgarten, K. Parvez, W. Pisula, S. De Feyter and K. Müllen, *J. Am. Chem. Soc.*, 2013, **135**, 13531–13537; (*b*) S. Xiao, S. J. Kang, Y. Zhong, S. Zhang, A. M. Scott, A. Moscatelli, N. J. Turro, M. L. Steigerwald, H. Li and C. Nuckolls, *Angew. Chem., Int. Ed.*, 2013, **52**, 4558–4562; (*c*) Y. Yamamoto, T. Fukushima, Y. Suna, N. Ishii, A. Saeki, S. Seki, S. Tagawa, M. Taniguchi, T. Kawai and T. Aida, *Science*, 2006, **314**, 1761–1764; (*d*) J. Cao, Y.-M. Liu, X. Jing, J. Yin, J. Li, B. Xu, Y.-Z. Tan and N. Zheng, *J. Am. Chem. Soc.*, 2015, **137**, 10914–10917.

4 C. Zhang, Y. Liu, X.-Q. Xiong, L.-H. Peng, L. Gan, C.-F. Chen and H.-B. Xu, *Org. Lett.*, 2012, **14**, 5912–5915.

5 (*a*) V. Vij, V. Bhalla and M. Kumar, *ACS Appl. Mater. Interfaces*, 2013, **5**, 5373–5380; (*b*) P.-C. Zhu, L.-N. Luo, P.-Q. Cen, J.-T. Li and C. Zhang, *Tetrahedron Lett.*, 2014, **55**, 6277–6280.

6 (*a*) Y. Liu, C.-F. Ke, H.-Y. Zhang, J. Cui and F. Ding, *J. Am. Chem. Soc.*, 2008, **130**, 600–605; (*b*) F. J. M. Hoeben, M. Wolffs, J. Zhang, S. De Feyter, P. Leclere, A. P. H. J. Schenning and E. W. Meijer, *J. Am. Chem. Soc.*, 2007, **129**, 9819–9828; (*c*) Z.-Q. Li, Y.-M. Zhang, D.-S. Guo, H.-Z. Chen and Y. Liu, *Chem. – Eur. J.*, 2013, **19**, 96–100.

7 W. W. H. Wong, T. Khoury, D. Vak, C. Yan, D. J. Jones, M. J. Crossley and A. B. Holmes, *J. Mater. Chem.*, 2010, **20**, 7005–7014.

8 J. M. Englert, J. Malig, V. A. Zamolo, A. Hirsch and N. Jux, *Chem. Commun.*, 2013, **49**, 4827–4829.

9 D. Lungerich, J. F. Hitzenberger, M. Marcia, F. Hampel, T. Drewello and N. Jux, *Angew. Chem., Int. Ed.*, 2014, **53**, 12231–12235.

10 J. Zhao, H.-Y. Zhang, H.-L. Sun and Y. Liu, *Chem. – Eur. J.*, 2015, **21**, 4457–4464.

11 H.-L. Sun, Y. Chen, J. Zhao and Y. Liu, *Angew. Chem., Int. Ed.*, 2015, **54**, 9376–9380.

12 (*a*) R. Kabe, X. Feng, C. Adachi and K. Müllen, *Chem. – Eur. J.*, 2014, **9**, 3125–3129; (*b*) J. M. Englert, F. Hauke, X. Feng, K. Müllen and A. Hirsch, *Chem. Commun.*, 2010, **46**, 9194–9196.

13 (*a*) K. Kano, R. Nishiyabu, T. Asada and Y. Kuroda, *J. Am. Chem. Soc.*, 2002, **124**, 9937–9944; (*b*) G. Liu, X. Xu, Y. Chen, X. Wu, H. Wu and Y. Liu, *Chem. Commun.*, 2016, **52**, 7966–7969.

14 (*a*) Q. Zhang, H. Peng, G. Zhang, Q. Lu, J. Chang, Y. Dong, X. Shi and J. Wei, *J. Am. Chem. Soc.*, 2014, **136**, 5057–5064; (*b*) J. Yu, Y. Chen, Y.-H. Zhang, X. Xu and Y. Liu, *Org. Lett.*, 2016, **18**, 4542–4545.

15 (*a*) Y. S. Cohen, S. Xiao, M. L. Steigerwald, C. Nuckolls and C. R. Kagan, *Nano Lett.*, 2006, **6**, 2838–2841; (*b*) A. A. Gorodetsky, C.-Y. Chiu, T. Schiros, M. Palma, M. Cox, Z. Jia, W. Sattler, I. Kymissis, M. Steigerwald and C. Nuckolls, *Angew. Chem., Int. Ed.*, 2010, **49**, 7909–7912.

16 (*a*) Z.-Y. Gu, D.-S. Guo, M. Sun and Y. Liu, *J. Org. Chem.*, 2010, **75**, 3600–3607; (*b*) K. Kilsa, J. Kajanus, J. Martensson and B. Albinsson, *J. Phys. Chem. B*, 1999, **103**, 7329–7339.

17 (*a*) Y. Chen, D. Zhao and Y. Liu, *Chem. Commun.*, 2015, **51**, 12266–12269; (*b*) X. Xiong, L. Gan, Y. Liu, C. Zhang, T. Yong, Z. Wang, H. Xu and X. Yang, *Nanoscale*, 2015, **7**, 5217–5229.

18 (*a*) X.-W. Liu, Y.-M. Shen, J.-S. Shu, Y. Xiao, S.-B. Zhang and J.-L. Lu, *J. Fluoresc.*, 2015, **25**, 1527–1535; (*b*) H. Kumar, V. Devaraji, R. Prasath, M. Jadhao, R. Joshi, P. Bhavana and S. K. Ghosh, *Spectrochim. Acta, Part A*, 2015, **151**, 605–615.

